

# Complex impedance analysis and magnetoelectric effect in composite $\text{BaSrTiO}_3\text{-NiZnFe}_2\text{O}_4$ ceramics

Vishal Khatri<sup>1</sup>, Vinay Kumar<sup>2</sup>, Ashwani Kumar<sup>3</sup>, Amit Sanger<sup>4</sup> and Renu Rani<sup>5\*</sup>

<sup>1</sup>Nalanda College of Engineering, Chandi, Nalanda, Bihar, India- 803108

<sup>2</sup>COBS&H, CCS Haryana Agricultural University, Hisar, Haryana, India- 125004

<sup>3</sup>Nanoscience Laboratory, Institute Instrumentation Centre, IIT Roorkee, Roorkee, 247667, India.

<sup>4</sup>Shriram Institute for Industrial Research, 19 University Road, New Delhi, 110 007, India

<sup>5</sup>Magadh University, Bodhgaya-824234

## Abstract

In the present study, high temperature solid state reaction method has been utilized to synthesize the composite  $\text{Ba}_{0.9}\text{Sr}_{0.1}\text{TiO}_3$  and  $\text{Ni}_{0.8}\text{Zn}_{0.2}\text{Fe}_2\text{O}_4$  (wt ratio 100:00 to 85:15). X-ray diffraction technique was used to confirm the formation of single-phase crystal system. Complex impedance spectroscopy (CIS) was used to investigate the electrical properties of composites. The variation of imaginary part of the complex impedance with frequency shows the Debye like relaxation behavior in the present samples. Additionally, the variation of ac conductivity as a function of temperature and frequency suggest that conduction process in the material is thermally activated. The activation energy has been obtained from the temperature variation of relaxation time and dc conductivity.

**Keywords:** Solid state reaction; XRD; Complex impedance spectroscopy; Electrical properties; activation energy.

## 1. Introduction

Impedance spectroscopy has been applied for a number of ferroelectric materials and dielectric substances. It is an important tool used for studying the electrical properties of polycrystalline materials. The solid electrode interface, grains and grain boundaries play a major role in electric properties of polycrystalline ceramics [1,2]. Ac technique can be adopted for proper estimation of electric conductivity. Complex impedance analysis helps to estimate the grains, grain boundaries and impurity phase if any, contributions towards the conductivity [3]. Thus, this study helps us to interoperate the proper conduction phenomenon. Much interest has recently

been generated in the composite material consisting of ferroelectric and ferromagnetic phase and have been exploited for applications like sensors, waveguides, switches, phase invertors etc. [4, 5]. In composites, the study of electrical conductivity is very important because various factors like conductivity of the constituent phase affect the magnitude of the electric polarization obtained [6, 7]. Work on impedance study of composite sample has hardly been found in the literature. Considering the fact, we are here to propose our research work on complex impedance analysis in  $(1-y)\text{Ba}_{0.9}\text{Sr}_{0.1}\text{TiO}_3 + (y)\text{Ni}_{0.8}\text{Zn}_{0.2}\text{Fe}_2\text{O}_4$  composite. In this work  $\text{Ba}_{0.9}\text{Sr}_{0.1}\text{TiO}_3$  is selected as a ferroelectric

\*Corresponding Author (Email: renudhy@gmail.com)

phase since it has a high dielectric constant, comparatively lower dielectric loss and curie temperature, which varies with the concentration of strontium[8] and the spinel  $\text{Ni}_{0.8}\text{Zn}_{0.2}\text{Fe}_2\text{O}_4$  has been selected as a ferrite phase since, it possesses a high resistivity and low eddy current losses, due to which it can be utilized for high frequency application in telecommunication[9]. The saturation magnetization of nickel ferrite increases with zinc content hence its magnetoelectric coefficient increases.  $\text{MnO}_2$  was added to minimize the hopping mechanism of  $\text{Fe}^{2+} \leftrightarrow \text{Fe}^{3+}$  which results in an increased resistivity of the samples[10].

## 2.Experimental

The ferrite and ferroelectric phases of the samples were synthesized by the conventional solid-state reaction. AR grade  $\text{NiO}$ ,  $\text{ZnO}$ ,  $\text{Fe}_2\text{O}_3$  were used as starting materials for the synthesis of ferrite phase. Ball-milling was done using zirconia balls with the distilled water as the milling media were used to mix the constituent materials. The resulting product was then dried and calcined in an alumina crucible at  $1000^\circ\text{C}$  for 4 hrs. A small quantity (0.5% by weight) of  $\text{MnO}_2$  was added to the resulting powder, ball milled and recalcined at  $1000^\circ\text{C}$  for 4 hrs. The recalcined powder was then ball milled again and dried. The ferroelectric phase was synthesised using the same technique, using AR grade  $\text{BaCO}_3$ ,  $\text{SrCO}_3$  and  $\text{TiO}_2$  as raw materials and calcined at  $1100^\circ\text{C}$ . Synthesis of the composites was carried out by mixing 0,5,10,15 % by wt.  $\text{Ni}_{0.80}\text{Zn}_{0.20}\text{Fe}_2\text{O}_4$  (NZF) phase to the  $\text{Ba}_{0.90}\text{Sr}_{0.10}\text{TiO}_3$  (BST) phase. Ball-milling of the constituents using zirconia balls was carried out with distilled water as the milling media. The resulting

mix was dried and subsequently, a small quantity of diluted PVA solution was used as the binder. Uniaxial hydraulic press was used to press the material into pellets having a thickness of 2-3 mm and a diameter of 15 mm. The pellets were then sintered at  $1325^\circ\text{C}$  for 4 hrs with a heating rate of  $5^\circ\text{C}/\text{min}$ . The structural characterization of the samples was done by using the X-ray diffractometer using  $\text{Cu-K}\alpha$  radiation ( $\lambda=1.541\text{\AA}$ ). For electrical measurement, silver paste was used to make ohmic contacts on the samples, followed by heating in an oven at  $400^\circ\text{C}$  for 1 hr. The dielectric measurements were performed as a function of frequency at different temperatures by using 4284A LCR meter interfaced to PC and programmable temperature chamber.

## 3.Results and discussion

The X-ray diffraction (XRD) patterns for the samples are depicted in Fig. 1. The pattern shows well defined peaks with specific indices, which are a characteristic of the perovskite type structure in the ferroelectric phase. The co-existence of the ferrite phase and ferroelectric phase is confirmed in composite sample. The intensity of the ferrite phase peak increases with the increase of ferrite content. It is seen that there is shifting of peaks towards lower angle in case of composite which indicates that there is change of lattice parameter for the ferroelectric phase. Since the growth of individual phases exerts stress on each other's crystal lattice and therefore, we expect a small change in the obtained lattice parameter of ferroelectric phase in composite sample [11, 12].

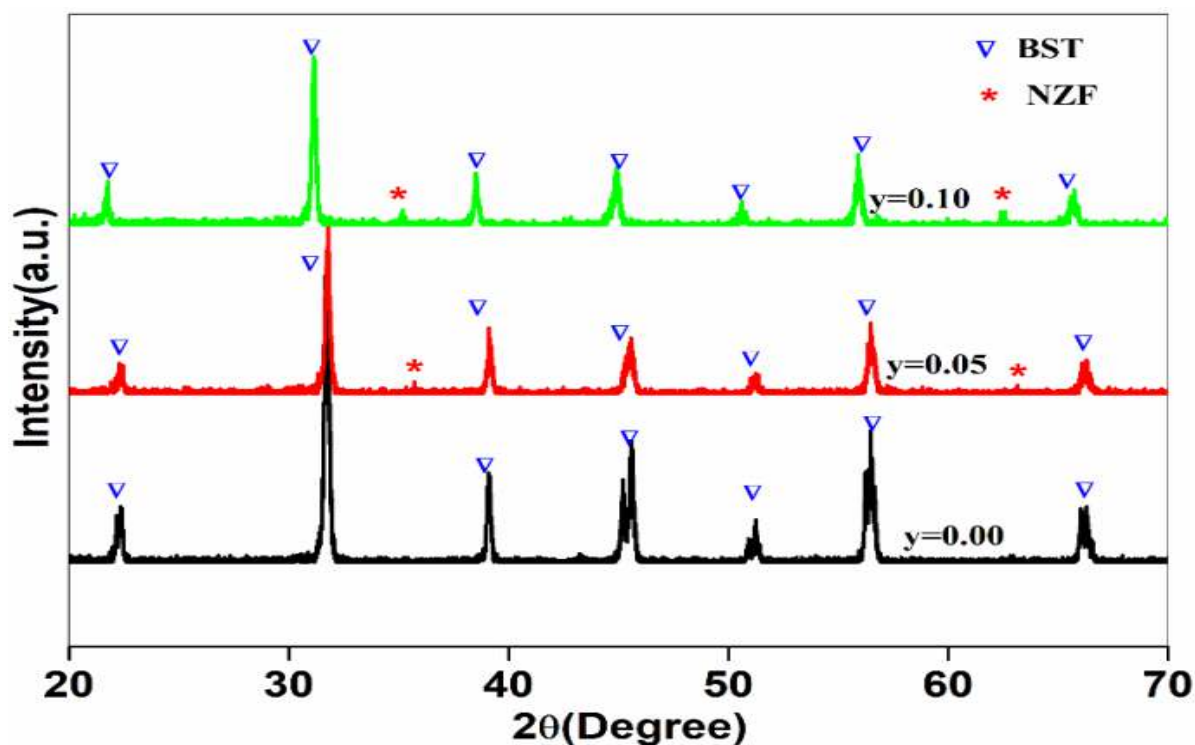


Fig. 1. XRD patterns for the different composition samples

The impedance data can be analyzed in terms of four complex formalisms, the complex dielectric constant ( $\epsilon^*$ ), the complex impedance ( $Z^*$ ), the electrical modulus ( $M^*$ ) and the dielectric loss ( $\tan\delta$ ). They are related to each other as [13, 14]

$$Z^* = Z - jZ'' = R - 1/j\omega C$$

$$\epsilon^* = \epsilon' - j\epsilon''$$

$$M^* = M' + jM'' = j\omega C_0 Z^*$$

Where  $\omega$  represents the angular frequency and  $C_0$  is the capacitance in free space. Complex impedance plot at particular temperature ( $450^\circ\text{C}$ ) for all samples are shown in Fig. 2. Characteristically two overlapping semicircle arcs were observed for all the samples. The diameter of the semicircle arc gives additional information

for calculating the grain resistance, grain boundary resistance, grain capacitance and grain boundary capacitance. The value of all these are given in Table 1. It is found that the bulk resistance and grain boundary resistance decreases with the addition of ferrite content. This suggests that the addition of ferrite phase leads to an enhancement in conductivity of the samples. It is also found that the grain boundary resistance is large as compared to the grain resistance. This is because, in ceramics methods cooling of samples is followed by sintering. Which results in re-oxidation and re-oxidation is restricted to the surface and grain boundaries because the diffusion of oxygen into the bulk does not happen due to the decreasing temperature and lack of sufficient time. Due to this, the grain boundaries are more insulating as compared to grain.

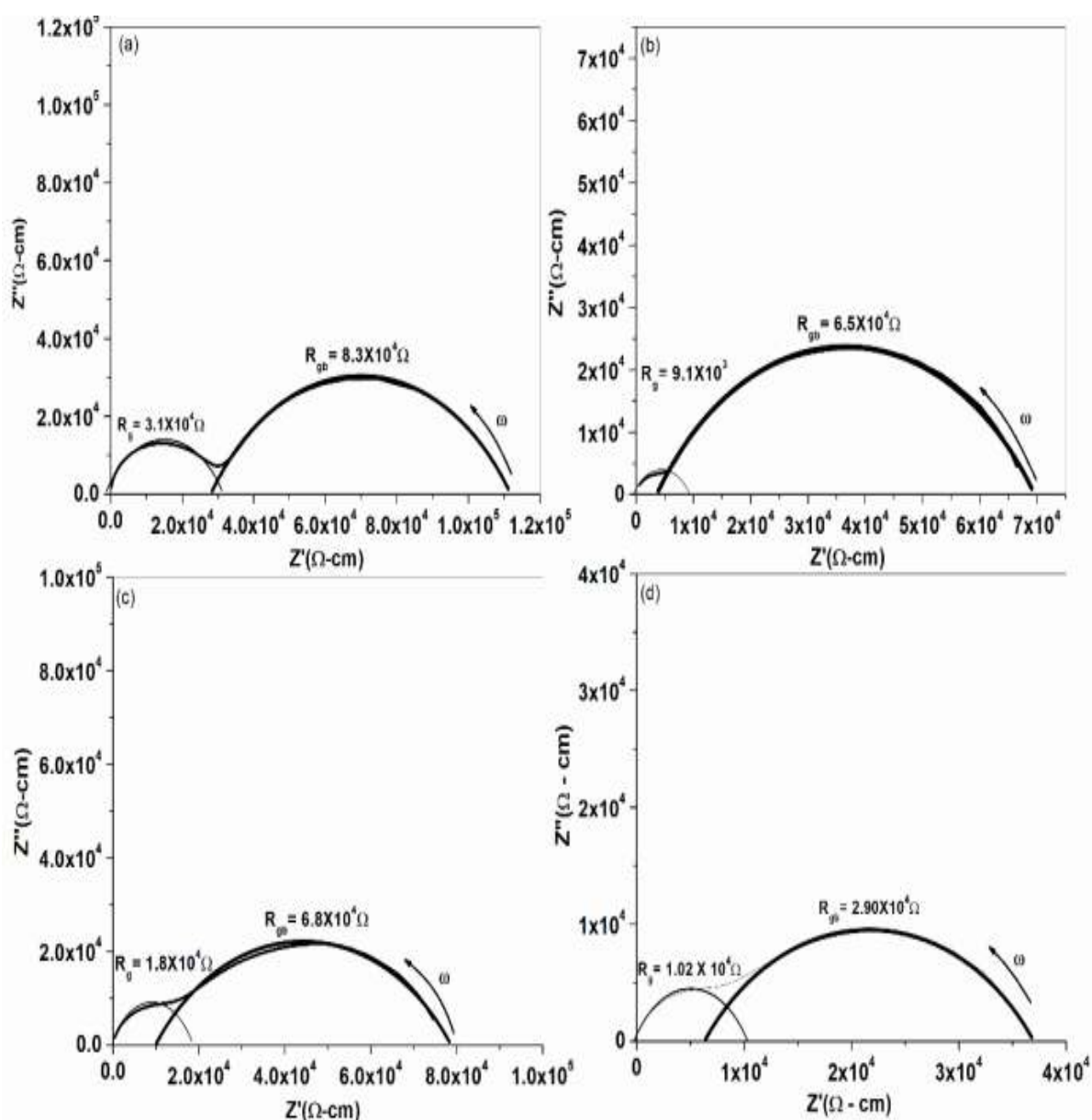


Fig. 2: Variation of real and imaginary part of impedance at 450°C for samples (a)  $y=0.0$  (b)  $y=0.05$  (c)  $y=0.10$  (d)  $y=0.15$

In Fig. 3 the variation of imaginary part of impedance ( $Z''$ ) with frequency at different temperature for  $y = 0.00$  and  $y = 0.15$  is shown. It is observed that all the curves attained a maximum value at a particular frequency for all different temperatures and appear to combine into a single curve in the higher frequency region. Similar behavior

was observed in the frequency dependent plots at different temperature for all other samples also. From graph it can be observed that for pure sample the low frequency peaks are observed at above 400°C. This can be attributed to the strong grain boundary effects in pure sample. A relative

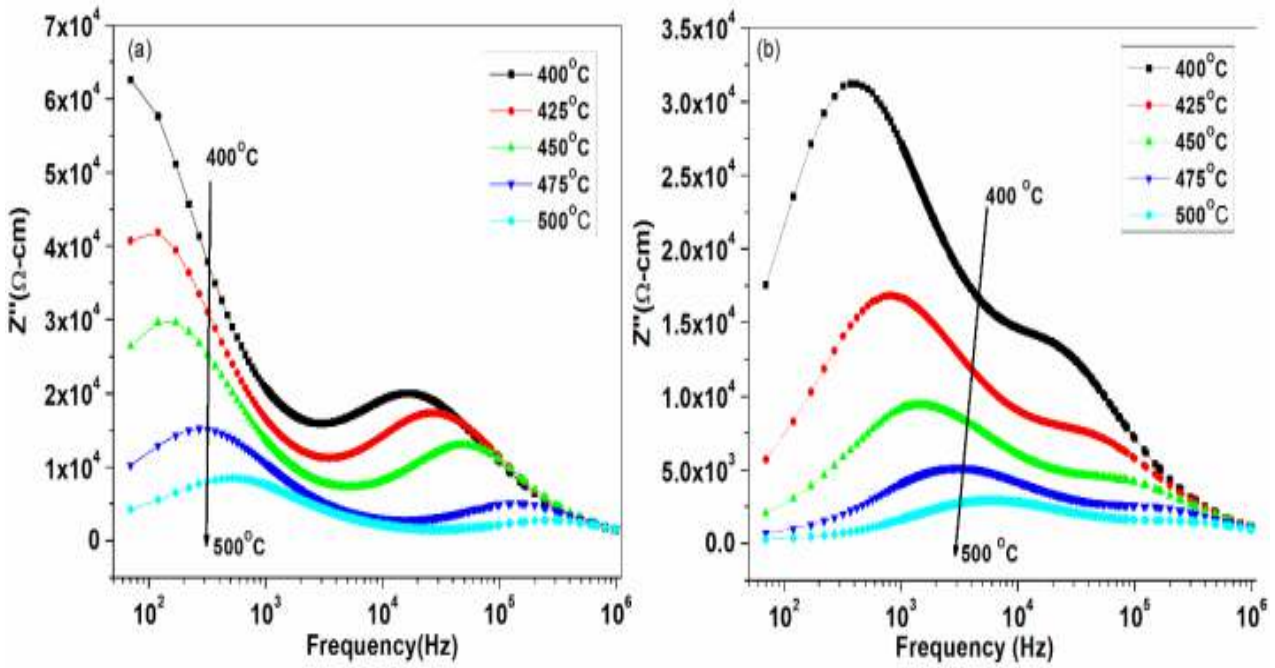


Fig. 3: Imaginary part ( $Z''$ ) of impedance as a function of frequency for samples (a)  $y=0.00$  (b)  $y=0.15$

lowering of the magnitude of  $Z''$  is observed with the addition of ferrite phase this is the indication of space charge domination that may develop at the interface of the two phases [15, 16].

The relaxation time  $\tau$  associated with the dielectric relaxation is calculated from the  $Z''$  vs frequency graph with the help of the relation:

$$\tau = 1 / 2\pi f_r$$

where  $f_r$  is the relaxation frequency

They follow the Arrhenius relation [17]

$$\tau = \tau_0 \exp(-E_\tau / K_B T)$$

Where  $\tau_0$  is the pre exponential factor,  $E_\tau$  is the activation energy and  $K_B$  is the Boltzmann constant.

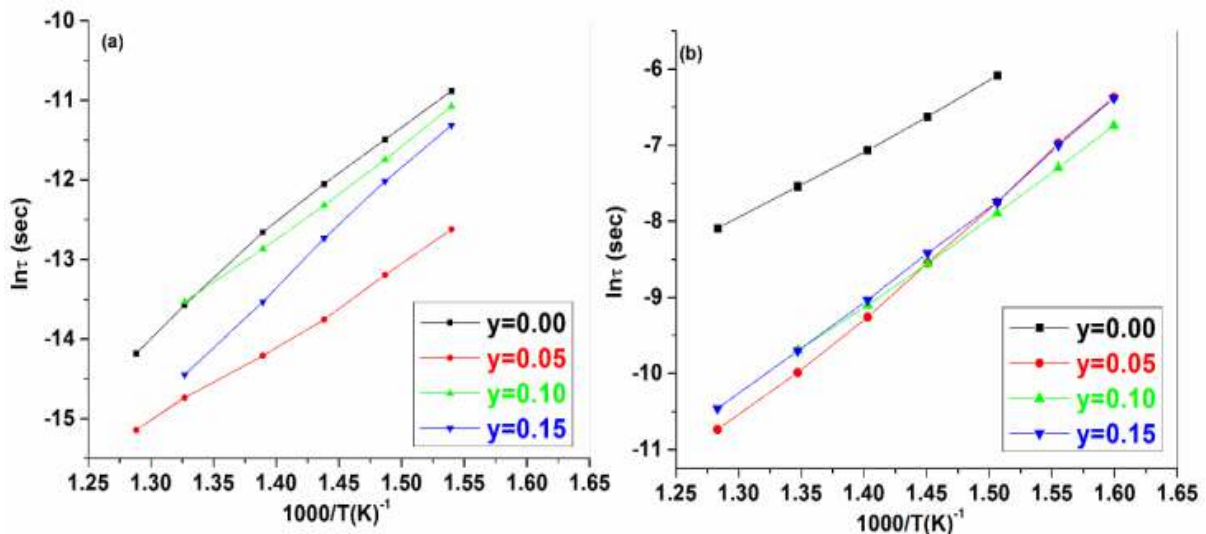


Fig. 4 Variation of relaxation time with inverse of temperature for samples (a) grain (b) grain boundary

The value of the activation energy evaluated from the slop of graphs is given intable 1 for all samples. The activation energy increases

with addition of ferrite. So, conducting ferrite phase effect the charge relaxation.

**Table 1: Activation energy, resistance and capacitance of grain and grain boundaries of different composition obtained from impedance and modulus plots**

y	E <sub>act</sub> (g) (eV)	E <sub>act</sub> (gb) (eV)	E <sub>τ</sub> (eV)	R <sub>g</sub> (kohm) at 450°C	R <sub>gb</sub> (kohm) at 450°C	C <sub>g</sub> (pf)	C <sub>gb</sub> (nf)
0.00	0.86	1.06	0.76	31	83	102	11
0.05	0.99	1.60	1.20	9	65	58	1.8
0.10	0.98	1.47	1.01	18	68	162	1.9
0.15	0.90	1.32	1.10	10	29	130	4.2

At higher temperature, the bulk and grain boundary dc conductivity of the compounds has been evaluated from the impedance data.

The typical variation of dc conductivity for grain and grain boundary is shown in Fig. 5.

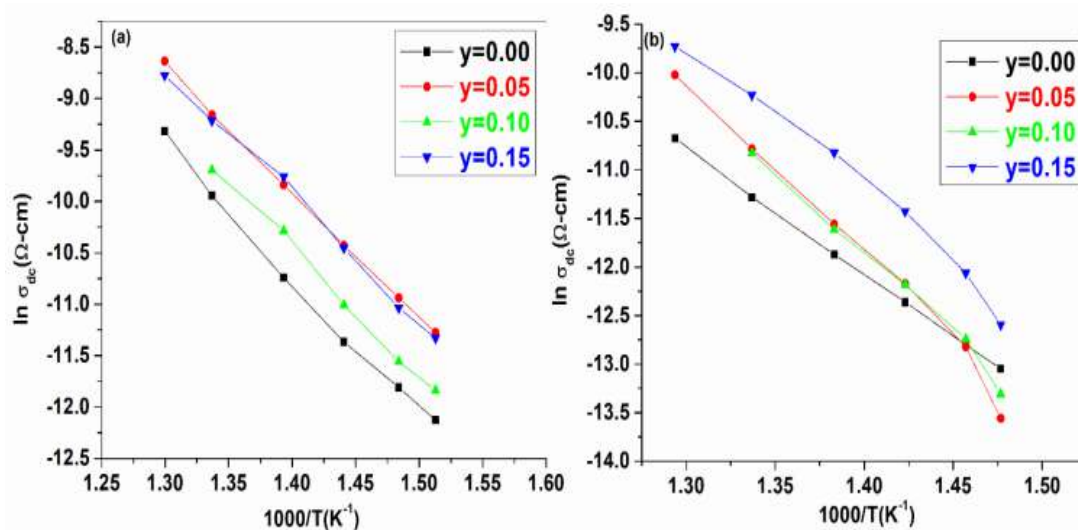


Fig. 5: Variation of dc conductivity with inverse of temperature for samples (a) grain (b) grain boundary

This shows that conductivity increases with addition of ferrite content. The dc conductivity plots also obey the Arrhenius law. The activation energy values for samples with different concentration of ferrite content calculated from the slope of the temperature vs conductivity plot are shown in Table1. The grain boundary

activation energy is found to be larger than the bulk activation energy. Fig. 6 shows the frequency dependence of ac conductivity of samples y = 0.00 and y = 0.15 at different temperature. The variation of ac conductivity with frequency is generally explained by using the universal law



$$\sigma(\omega) = \sigma'_{ac}(\omega) + \sigma_{dc}$$

$$\sigma'_{ac} = B \omega^s$$

Where B is constant,  $\sigma_{dc}$  is dc conductivity and s is exponent.

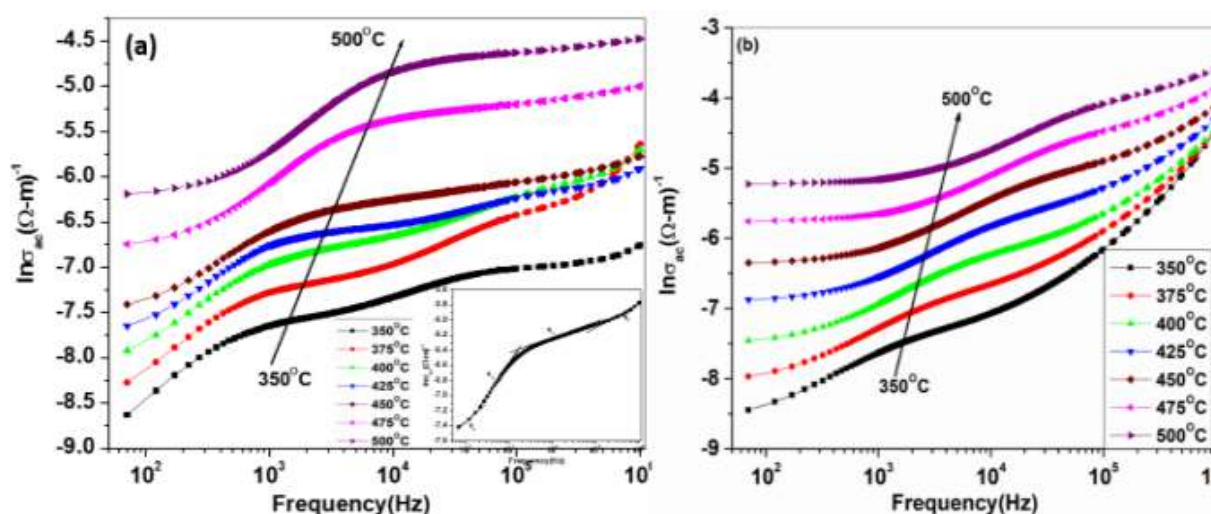


Fig. 6: Variation of ac conductivity with frequency at different temperatures for samples (a)  $y=0.0$  (b)  $y=0.15$

The exponent s is generally found to lie in the range of 0 to 1 for ionic conduction. But it is clear from the plots that results do not follow the simple power law relation as given above [18]. So power law cannot be used to describe the frequency dependence of ac conductivity in the present case because of appearance of two to four slopes in the measured frequency range.

Hence a four term power relation

$$\sigma'_{ac}(\omega) = \sigma_{dc} + B_1 \omega^{s_1} + B_2 \omega^{s_2} + B_3 \omega^{s_3} + B_4 \omega^{s_4}$$

is proposed to explain the variation of ac conductivity with frequency

The variation in the value of s may have a usual meaning, and has been explained by Funk,  $s \leq 1$  implies that the type of hopping motion is translational. Whereas, a value of larger than 1 would result in a motion that is localized hopping, i.e. remaining confined to the neighborhood [19]. The frequency at which there is a change in slope is known as the polaron hopping frequency. A significant dispersion in the variation of conductivity as a function of temperature was observed in the low frequency region and allows appear

to merge in to single curve for higher frequencies but at low temperature.

#### 4. Conclusion

The co-existence of both phases in composite samples are confirmed from XRD. It is found that the bulk resistance and grain boundary resistance decreases with the addition of ferrite. Thus, it may be concluded that the conduction is dominantly due to the ferrite phase. The activation energy in grain boundary agree well with the values calculated using the relaxation time vs temperature plot. Due to the similarity in the values obtained for the two samples, we may conclude that the conduction process may be due to the same type of charge carriers.

#### Acknowledgement

The authors would like to thank the University Grant Commission, India ([No.F.30-445/2018 (BSR), F.D.Dy.No. 4854]) for financial support.

#### References

- [1] J.E. Baverle, J. Phys. chem. Solids 30 (1969) 2657.

- [2] L. Pandey , O. Prakash, R. Katare, D. Kumar, Bull. Mater. Sci. 18 (1995) 563.
- [3] N. Rammanohar Reddy, E. Rajagopal et.al., J. Electroceramics,11(2003)167.
- [4] C.W. Nan, L. Liu, N. Cai, J. Zhai, Appl. Phys. Lett., 81(2002) 20.
- [5] L.P.M. Bracke, R.G. Van Vliet, Int. J. Electron., 51 (1981) 225.
- [6] J.G. Wan, J-M. Liu, J. Appl. Phys., 93 (2003) 12.
- [7] H Abdelkefi, H khemakhem, G Velu, C Carru J. Alloys Compd. 399 (2005) 1
- [8] Y Cheng, Y Zheng, Y Waeng, F Bao and Y Qin 2005 J. Solid State Chem.1782394.
- [9] A.J. Moulson, J.M. Herbert, Electroceramics, Chapman and Hall, UK,1990.
- [10] A S Fawzi, A D Sheikh, V L Mathe, 2010 Phys. B 405 340.
- [11] K. Srinivas, P.Sarah, S.V. Suryanarayana, Bulletin of material science 26 (2003)247-253
- [12] J.R. Macdonald, Impedance spectroscopy , John wiley and sons, New York (1987)
- [13] J. Maier, J. European ceramic Society 24 (2004) 1343.
- [14] S. Sen, S.K.Mishra, S.K. Das, A. Tarafdar, J. Alloys and compounds 453 (2008)395.
- [15] S. Dutta, S. Bhattacharya, D.C. Agarwal, Material science eng B 100 (2003) 191-198
- [16] M. Vijayakumar, S. Selvasekharapandian, M.S. Bhuvneswari, G. Hirankumar, G.Ramprasad, R.Subramanian, P.C. Angelo, Physics B 334 (2003) 390-397.
- [17] K. Funke, Prog. Solid state chem. 22 (1993) 111-115